12C.6 **A STUDY ON THE LANDFALL TYPHOON WITH COMPACT STRUCTURE IN TAIWAN**

Yen-Chu Chen, Cheng-Shang Lee and Wei-Ting, Fang

Dept of Atmospheric Sciences, National Taiwan University, Taipei, Taiwan

1. INTRODUCTION

In 2001, Typhoon Toraji made landfall at Chin-Pu in eastern Taiwan at 1600 UTC 29 July and caused serious damages to the island. Toraji hit Taiwan with an estimated maximum sustained wind of 38 ms^{-1} (10-min-averaged wind) and a minimum mean sea level pressure (MSLP) of 962 hPa. In 2006, Typhoon Kaemi hit Taiwan with intensity comparable to Toraji at landfall (38 ms^{-1}, 960 hPa), but did not cause much damage. The landfall duration of Toraji (10 hours) is longer than that of Kaemi (5 hours). The 3-hourly rainfall distributions when Toraji and Kaemi just hit Taiwan are shown in Fig.1. Results show that the maximum 3-hourly rainfall is above 360 mm for Toraji, but it is only 80 mm for Kaemi. It is also interesting to note that the heavy rainfall for Toraji occurred only near the center with the heaviest rainfall occurred at Kuang-Fu located at 19.4 km away from the landfall point. In contrast, the relatively heavier rainfall for Kaemi occurred over a larger area.

As Toraji approached Taiwan, continuous radar coverage of the eyewall was provided by the radar network. The radar reflectivity images show that Typhoon Toraji appeared an extremely intense and compact structure (an example is shown in Fig.2a). Before making landfall, the deep convection of Toraji concentrates only within 25 km radius. As the typhoon made landfall, the deep convection caused heavy rainfall near the center as shown in Fig.1a. Such concentrated convection resulted in 146.5 mm (390 mm) maximum hourly (3-hourly) rainfall at a station nearby the landfall point. The radar reflectivity images of Kaemi (Fig.2b) show that before landfall the structure of Kaemi is more asymmetric than that of Toraji. Even if the area with strong reflectivity of Kaemi is larger than that of Toraji, the accumulated and maximum rainfall of Kaemi are still less than those of Toraji.

Observations at Chin-Pu (Fig.3), an automated station closed to the landfall point, show that the minimum pressure is 958.4 hPa. However, the station pressure increases rapidly (17 hPa in 3 hour) after the passage of typhoon center. The measured maximum wind speed reaches 25 ms^{-1}, and the hourly maximum rainfall exceeds 50 mm. However the measured wind speeds drop significantly at stations about 50 km north (Hualian) and south (Taitung) of Chin-Pu. The wind speeds drop from 25 ms^{-1} at 5 km radius from the center to 12 ms^{-1} at 50 km radius from the center. Another important issue is the track deflection before typhoon landfall in Taiwan. Four hours before Toraji made landfall, there is a noticeable track deflection (Fig.1). The moving direction of Toraji shifts from north-northwestward to west-northwestward, resulting in a 100 km southward

Corresponding author address: Yen-Chu Chen, Department of Atmospheric Sciences, National Taiwan University, e-mail:deliachen@ntu.edu.tw

shift of the landfall point.

On the other hand, using the QuikSCAT data we have analyzed size change (radius of 15 ms^{-1} tangential wind) for Tropical cyclones (TCs) in the western North Pacific (WNP) during 2000-2005. Results show that if a TC's size is relatively large (small) when it develops to tropical storm (TS) intensity; it has 70% (65%) of possibility to remain as a large (small) TC when it intensified to typhoon (TY) stage. In other word, a TC tends to retain its size category during the developing phase from TS to TY. Therefore, it is interesting to see how the Taiwan topography would affect the size of a typhoon when it made landfall in Taiwan, especially for a typhoon with compact structure like Toraji. It is also interesting to see how well the model (WRF) can simulate the landfall process of a typhoon with compact structure, especially the track deflection and the concentrated rainfall distribution. In the presented study, we will show some preliminary analysis regarding the landfall typhoons with compact structure in Taiwan. The data analysis of compact typhoons is presented in section 2. Section 3 is the model simulation and analysis. Summary and conclusion are presented in section 4.

2. ANALYSIS OF TYPHOON WITH COMPACT STRUCTURE

To better describe the structure of a TC, Holland and Merrill (1984) defined a parameter, strength which is different from the conventionally used intensity and size. Although intensity, strength and size can be used to describe the structure of a TC, it is not suitable enough for this study. Thus we define a new parameter which can be used as a measure of how compact a typhoon is.

Previous studies (Weatherford and Gray 1988) have shown that a stronger TC tends to have a smaller eyewall radius or a radius of maximum tangential wind (R_{max}). For a compact TC, however, the R_{max} would be smaller than what is expected itself using such relationship for a given vortex. Therefore, a TC is considered to be compact if (1) the tangential wind speed (Vt) decreases greater than what is expected for a general TC outside the R_{max}, (2) the R_{max} is smaller than what is expected for a general TC for a given maximum tangential wind speed (Vt_{max}). A structure parameter S is thus defined as follow:

$$S = \frac{\mathrm{V}t_{\mathrm{S}}}{\mathrm{V}t_{\max}} \times \frac{\left(R_{\max} \times \mathrm{V}t_{\max}\right)}{\left(RVt\right)_{ave}} = \mathrm{V}t_{\mathrm{S}} \times \frac{R_{\max}}{\left(RVt\right)_{ave}} ,$$

Where Vt_S is the tangential wind speed at the two times of the R_{max} (Fig.4), $(RVt)_{ave}$ is an average value taken from the real cases. For a compact TC, S parameter should be relatively small.

To illustrate how parameter S change for TCs with different structures, Rankine vortex is used to define some idealized cases and then calculate the S value for each case (Table 1). Here the tangential wind for a Rankine vortex is given by

$$\mathrm{V}t(r) = \mathrm{V}t_{\max}\left(\frac{r}{R_{\max}}\right) , \quad 0 < r \le R_{\max} ,$$

$$\mathrm{V}t(r) = \mathrm{V}t_{\max}\left(\frac{R_{\max}}{r}\right)^{\alpha} , \quad R_{\max} \le r ,$$

The alpha value decides the tangential wind speed profile outside the R_{max}. It is easy to perceive that the large alpha value leads to a small S parameter (Table 1, Exp.A). By fixing Vt_{max} and alpha value, we can expect that the smaller R_{max} would be accompanied by smaller S parameter (Table 1, Exp.R). In the experiment V, with the same R_{max} and alpha value, the smaller value of Vt_{max} has a smaller S parameter (Table 1, Exp.V). The results satisfy the argument which we mentioned before.

To apply the S parameter to the real cases, the QuikSCAT 10-m winds are used for each typhoon that moved westward and affected Taiwan in 1999~2007. After eliminating the cases with concentric eyewalls, there are only four cases for further analysis. The tracks of these four typhoons are shown in Fig.5. Except Longwang (2005), other typhoons came from the southeast of Taiwan and made landfall on the east coast of the island. The MSLP of these typhoons are: 962 hPa (Toraji, 2001), 925 hPa (Longwang, 2005), 960 hPa (Kaemi, 2006) and 920 hPa (Sepat, 2007).

Due to the limitation of QuikSCAT observation, the number of time passes with better data coverage is limited. Therefore, Fig.6 shows the QuikSCAT wind pattern for each typhoon with the best quality of observation before landfall. Results show that Longwang (Fig.6b) appears to be highly symmetric when compared to other cases. In Fig.6a, Toraji is closed to the landfall point, so the wind pattern is influenced by the Taiwan terrain. Using data shown in Fig.6, we calculate tangential wind speed for each case (Fig.7). The S parameters then are calculated for each case (Table 2). Base on our agreement, Typhoon Toraji (2001) is the most compact system among these four cases. Typhoon Sepat (2007) has the most non-compact structure. However, S parameter does not mean that Sepat is the weakest or the most unorganized typhoon.

According to the typhoon's MSLP, these typhoons can be divided into two groups (Toraji v.s. Kaemi and Longwang v.s. Sepat). Thus we can discuss the typhoon structure with similar intensity. The S parameters show that Toraji and Longwang are considered to be the compact typhoons and will be simulated in the following study. For Toraji, the observed rainfall and radar reflectivity have been presented in section 1.

The 2005 typhoon season was quite a special year to Taiwan, there were three super typhoons (STY) invaded Taiwan. Longwang was the third STY. Before Longwang made landfall on Taiwan, there was the first eyewall penetration by the Aerosonde (Lin and Lee 2008). We use such valuable data to analyze the structure of Longwang. Using the Aerosonde inbond data, we calculate the tangential wind profile (Fig.8). Results show that the Vt_{max} is 55 ms^{-1} with the R_{max} at 30 km. The Aerosonde estimated minimum center pressure (920 hPa) is very closed to the CWB warning report (925 hPa). Outside the R_{max}, tangential wind profile is also similar to the QuikSCAT tangential wind profile. The difference between these two measurements is larger at radii of 150 to 200 km which is caused by a deep convective rainband. Since this is only a flight-leg data, it is hard to compare Aerosonde measurements with other results using QuikSCAT winds. However, the S parameter calculated by using Aerosonde data (0.52) implies that before landfall, the structure of Longwang become more compact when compared to the S parameter calculated by using QuikSCAT data (0.65).

3. MODEL SIMULATION AND ANALYSIS

Since a compact TC tends to post greater threat to a small area, the track prediction or the landfall point forecast appears to be an extremely important issue. Thus it is highly desired to see how the model can perform for such compact TC. The modeling system used here is the Weather Research and Forecasting Model Version 2.2 (WRF Model) (Skamarock et al. 2005). The model contains four nested domains, with grid spacings of 54 km, 18 km, 6 km and 2 km with domain sizes of 141X141, 142X142, 199X199 and 241X241 grid points, respectively. Results show that different parameterization schemes would lead to different structures. The model physics used in the control run included Lin et al. microphysics scheme (Lin et al. 1983), Kain-Fritsch convective parameterization scheme (Kain and Fritsch,1993), YSU PBL scheme, Dudhia shortwave radiation scheme (Dudhia 1989) and the RRTM longwave radiation scheme (Mlawer et al.,1997). All the selected cases are simulated; unfortunately we can only have reasonably simulations for Longwang. Therefore, in the following we will illustrate only the simulated results of Longwang with special focus on the structural changes before landfall.

A comparison of the model-simulated and observed typhoon track and the rainfall distribution reveals that the model has simulated reasonably well, especially the major feature of rainfall distribution (Fig.9). It is worthy to mention that there is no bogusing of the storm at the initial time period in the control run and there is no continuous data assimilation as the simulation progressed. During the landfall period, heavy rainfall occurs to the north (Hualian County) of the typhoon track. Except that the model gives a slightly higher rainfall amount; the model-simulated rainfall pattern is almost identical to the observed.

Fig.10 shows the continuous radar observations before Longwang made landfall. The radar reflectivities show that there are several strong rainbands around the typhoon center. At the southwest quadrant, rainband extends outward from the eyewall. The rainbands rotate counterclockwise and merge into the eyewall. Besides, there is a rainband pass the northern part of Taiwan. The model-simulated reflectivities are also shown in Fig.10 (lower panel). Comparing the model-simulated reflectivities with observed reflectivities shows that the simulation reproduces the convective structure reasonable well. The only drawback is that the radius of the simulated eyewall is slightly larger than the radar observation.

The west-east vertical cross-section of the tangential wind speeds through the storm center for the control run is displayed at 1-h interval in Fig.11, from 4 hr before landfall (-4hr) to the landfall time (0hr). Results show that the typhoon structure is vertically aligned. When compared to the west side, strong wind speeds area (Vt > 40 ms^{-1}) on the east side extends higher levels (300 hPa). From -4hr to -3hr, the lower-level (750~950 hPa) maximum tangential wind speeds are shifted from the west side of the center to the east side of center.

In order to compare the model result with the

Aerosonde observation, we also calculate the S parameters which are shown in Table 3. Results show that the model calculated S parameter 0.50 (-7 hr) is very similar to the Aerosonde calculated S parameter (0.52). Table 3 also reveals that when typhoon is approaching Taiwan, the structure of the typhoon seems to become more compact, which is an interesting phenomenon and worth of further analysis.

4. SUMMARY AND CONCLUSION

The accuracy of typhoon track forecasts has improved steadily in recent years. At the same time, there has been comparatively little advance in predicting the tropical cyclones intensity change (DeMaria and Kaplan 1997). Furthermore, the simulation of structure characteristic is even more difficult. The typhoon structure is a complicated issue; it involves impacts in different scale's, such as environmental conditions, internal fluctuations, terrain impact …etc. In this study only one of four selected cases can simulate typhoon structure reasonably well. The reason might come from the shortage of observation data or the lack of model physical processes. We will improve our model simulation in order to analyze the process of TC maintain a compact structure. Furthermore, try to simulate different structure cases and identify the relation between compact structure and topography effect.

A new parameter which can be used as a measure to describe a compact typhoon is illustrated in this study. Compare with the Rankine vortex alpha value. The S parameter can give us specific information about the relation between Vt_{max} and R_{max}. We will apply this parameter to other real cases, try to find out the characteristic of compact structure typhoons.

Lessons drawn from the Typhoon Toraji told us that the now casting and warning operational organization should pay more attention on the compact structure typhoon. The heavier rainfall especially in a short time lag often brings huge disaster. In addition they always accompany with strong gust wind, it would threaten the human beings' safety even more.

5. REFERENCE

DeMaria, M., and J. Kaplan, 1997: An operational evaluation of a statistical hurricane intensity prediction scheme (SHIPS). *Preprints, 22d Conf. ON Hurricanes and Tropical Meteorology, Fort Collins, CO, Amer. Meteor. Soc.*, 280-281.

Dudhia, J., 1989: Numerical study of convection observed during the winter monsoon experiment using a mesoscale two-dimensional model, *J. Atmos. Sci.*, **46**, 3077-3107.

Holland, G. J. and R. T. Merrill, 1984: On the dynamics of tropical cyclone structural changes. *Quart. J. R. Met. Soc.*, **110**, 723-745

Kain, J. S., and J. M. Fritsch, 1993: Convective parameterization for mesoscale models: The Kain-Fritcsh scheme, The representation of cumulus convection in numerical models, K. A. Emanuel and D.J. Raymond, Eds., *Amer. Meteor. Soc.,* 246 pp.

Lin, P.-H., C.-S. Lee, 2008: The Eyewall-Penetration Reconnaissance Observation of Typhoon Longwang (2005) with Unmanned Aerial Vehicle, Aerosonde. *J. Atmos. Oceanic. Technol.*, **25**, 15-25.

Lin, Y.-L., R. D. Farley, and H. D. Orville, 1983: Bulk parameterization of the snow field in a cloud model. *J. Climate Appl. Meteor.*, **22**, 1065-1092.

Mlawer, E. J., S. J. Taubman, P. D. Brown, M. J. Iacono, and S. A. Clough, 1997: Radiative transfer for inhomogeneous atmosphere: RRTM, a validated correlated-k model for the longwave. *J. Geophys. Res.*, **102 (D14)**, 16663-16682.

Skamarock, W. C., J. B. Klemp, J. Dudhia, D. O. Gill, D. M. Barker, W. Wang, and J. G. Powers, 2005: A description of the Advanced Research WRF Version 2. *NCAR Tech. Note NCAR/TN-468+STR*, 88 pp.

Weatherford, C. L., and W. M. Gray, 1988b: Typhoon Structure as Revealed by Aircraft Reconnaissance. Part II: Structural Variability. *Mon. Wea. Rev.*, **116**, 1044-1056.

Exp	Vt_{max}	R_{max}	*alpha*	*S*
A1	40	80	0.5	1.00
A2	40	80	0.7	0.87
A3	40	80	0.9	0.76
R1	40	60	0.7	0.65
R2	40	80	0.7	0.87
R3	40	100	0.7	1.09
V1	30	80	0.7	0.65
V2	40	80	0.7	0.87
V3	50	80	0.7	1.09

Table 1 The S parameters calculate by idealized cases. Exp.A1~A3 changes *alpha* value, Exp.R1~R3 changes R_{max} (km) value and Exp.V1~V3 changes Vt_{max} (ms^{-1}) value.

Case	R_{max}	Vt_{max}	Vt_S	*S*	*Data*
Toraji(2001)	76.2	27.6	13.5	0.46	QSCAT
Longwang(2005)	101.6	34.6	14.3	0.65	QSCAT
Longwang(2005)	30.4	51.6	38.0	0.52	Aerosonde
Kaemi(2006)	98.4	32.3	12.5	0.55	QSCAT
Sepat(2007)	72.4	36.7	23.3	0.75	QSCAT

Table 2 The S parameters calculate by real cases. (R_{max} in km, Vt_{max} and Vt_S in ms^{-1})

Time	R_{max}	Vt_{max}	Vt_S	*S*
-7 hr	48.7	46.8	22.9	0.50
-6 hr	46.2	42.6	25.8	0.53
-5 hr	36.3	42.8	29.4	0.48
-4 hr	33.7	47.1	30.4	0.46
-3 hr	38.3	48.2	27.8	0.48
-2 hr	51.3	48.5	18.9	0.43
-1 hr	20.3	50.0	34.4	0.31

Table 3 he S parameters calculate by Longwang model simulation. Time is compared with landfall time. (R_{max} in km, Vt_{max} and Vt_S in ms^{-1})

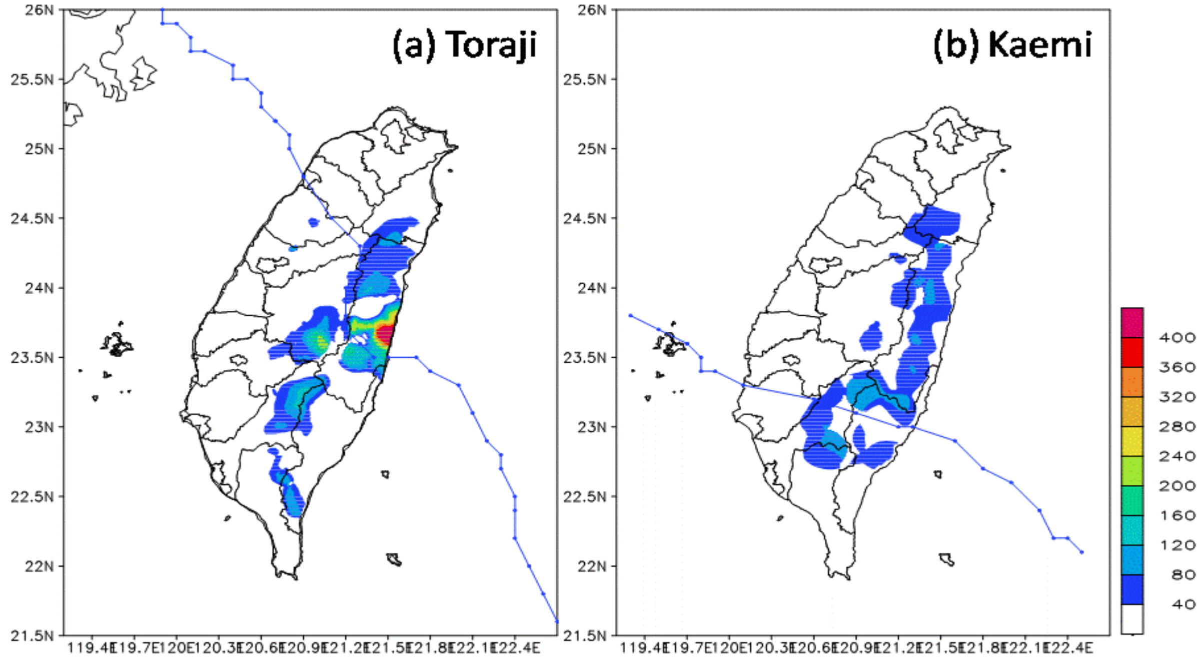

Fig. 1 Accumulate rainfall and Typhoon best track. (a) Toraji (2001) accumulate rainfall from 1600 UTC 29 Jul to 1800 UTC 29 Jul ,(b) Kaemi (2006) accumulate rainfall from 1500 UTC 24 Jul to 1700 UTC 24 Jul.

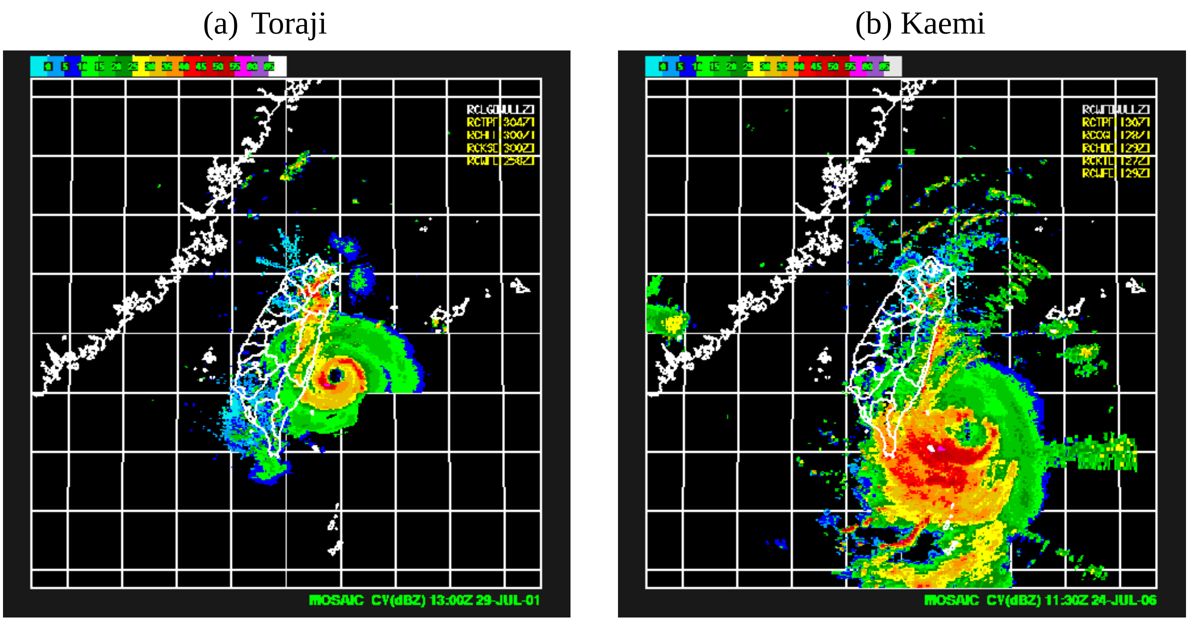

Fig. 2 CWB Composite of radar reflectivity(dBZ), (a) Typhoon Toraji (2001), 1300 UTC 29 Jul 2001, (b) Typhoon Kaemi (2006), 1130 UTC 24 Jul 2006. (Data source: CWB)

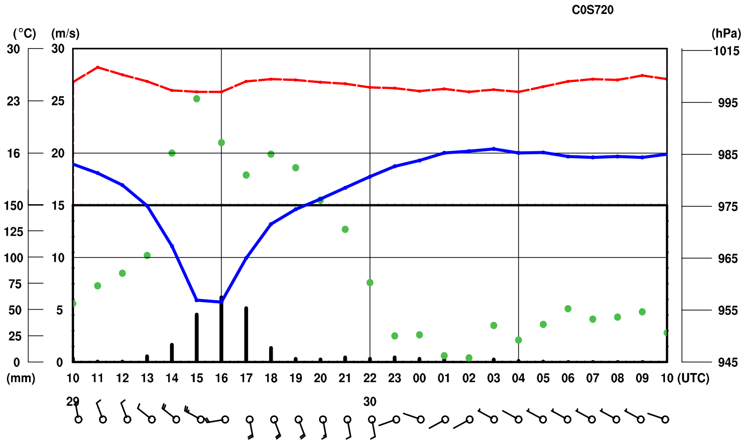

Fig. 3 Time series of automatic station data at Chin-Pu. Temperature in ℃ (red line), pressure in hPa (blue line), wind speed in ms^{-1} (green dot) and hourly rainfall in mm (bar).

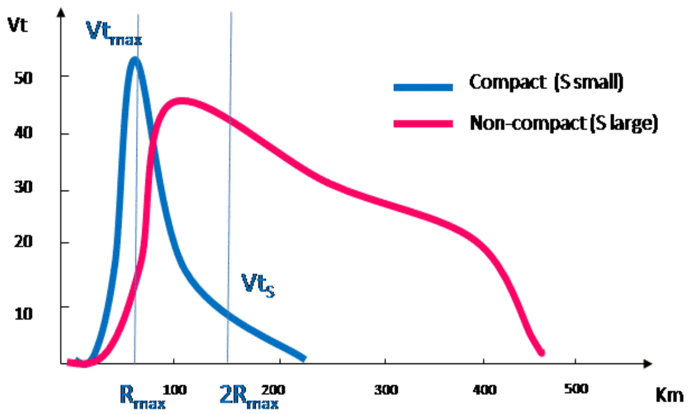

Fig. 4 The S parameter calculation definition.

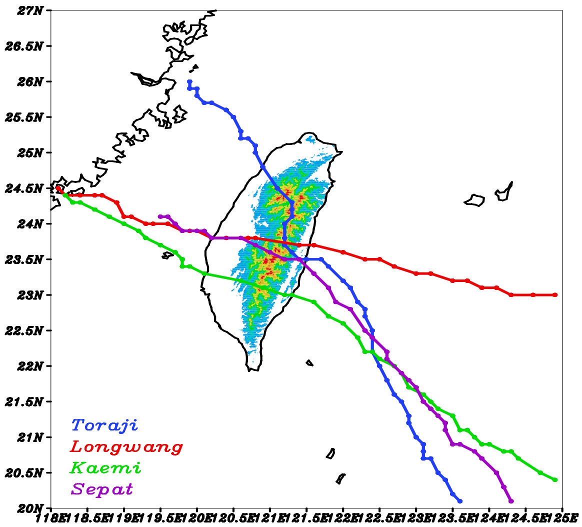

Fig. 5 Best tracks of selected typhoons, blue line is Toraji (2001), red line is Longwang (2005), green line is Kaemi (2006) and purple line is Sepat (2007). (Data source: CWB warning report)

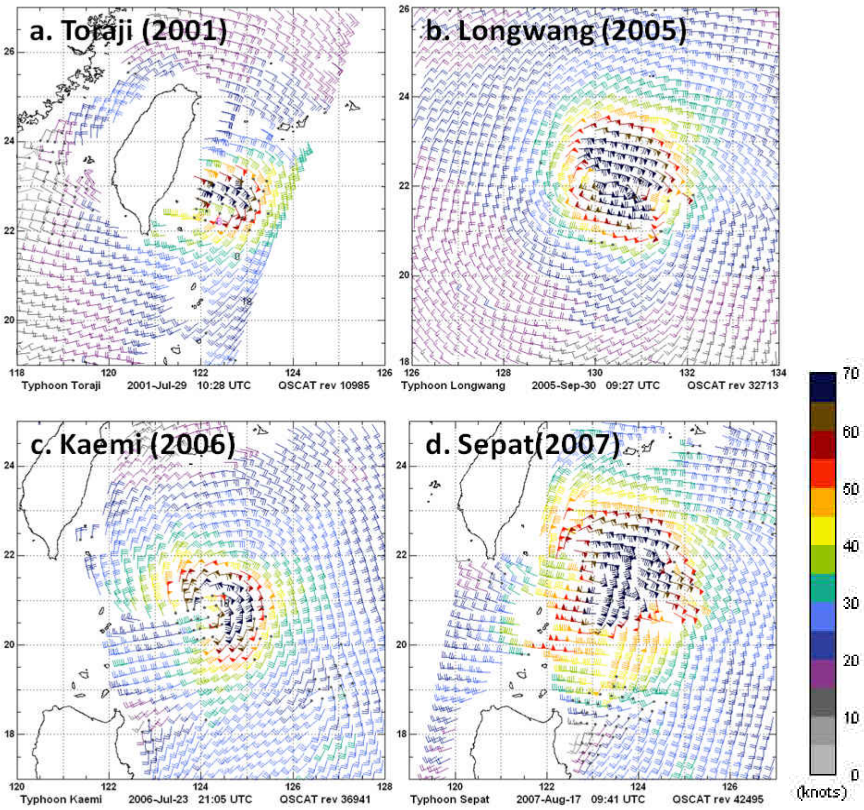

Fig. 6 QuikSCAT wind pattern of selected typhoons. (a) Toraji (2001), 1028 UTC 29 Jul, (b) Longwang (2005), 0927 UTC 30 Sep, (c) Kaemi (2006), 2105 UTC 23 Jul and (d) Sepat (2007), 0941 UTC 17 Aug. (Data source: http://www.remss.com/)

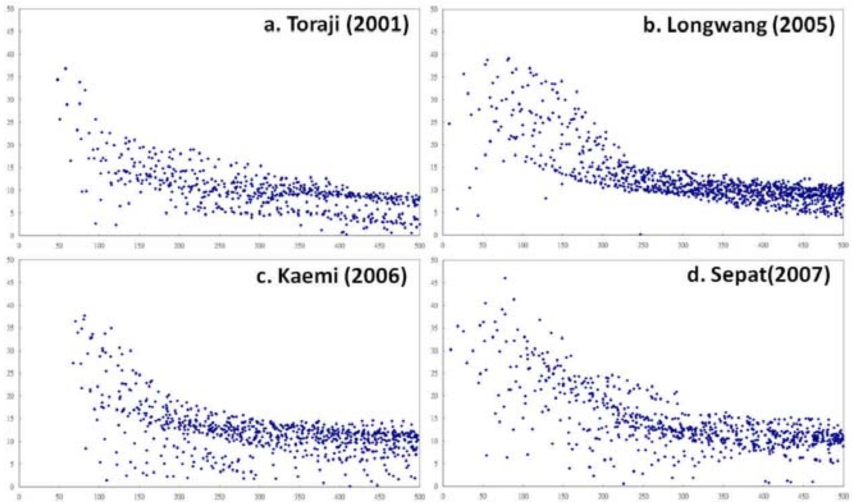

Fig. 7 QuikSCAT tangential wind speed profile of selected typhoons. x-axis represent the distance to the typhoon center (km), y-axis represent the tangential wind speed (ms^{-1}). (a) Toraji (2001), 1028 UTC 29 Jul, (b) Longwang (2005), 0927 UTC 30 Sep, (c) Kaemi (2006), 2105 UTC 23 Jul and (d) Sepat (2007), 0941 UTC 17 Aug. (Data source: http://www.remss.com/)

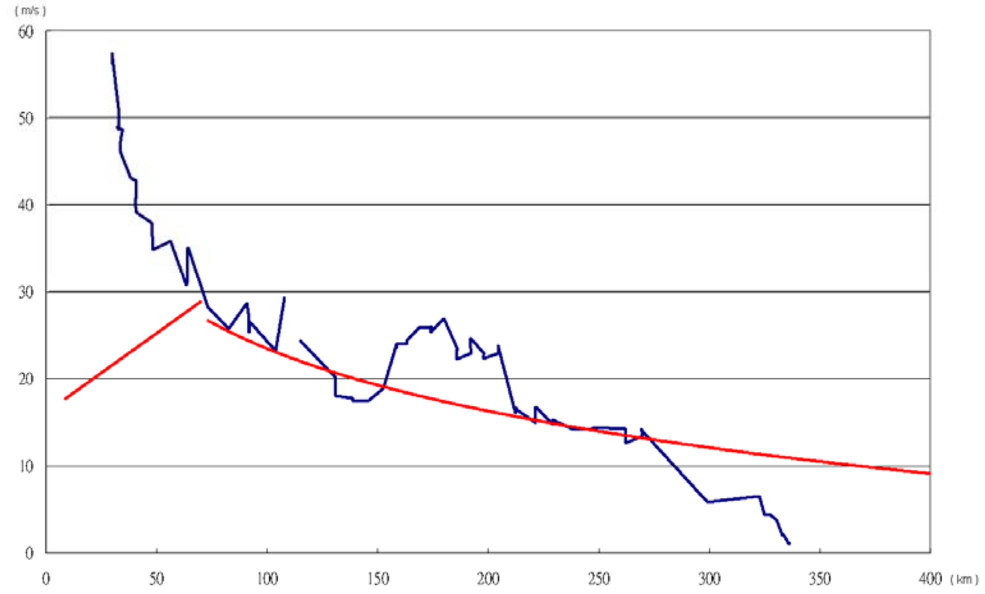

Fig. 8 Longwang (2005) tangential wind speed profile. QuikSCAT data at 0927 UTC 30 Sep (red line) and Aerosonde data at 1400 UTC 01 Oct (blue line). x-axis represent the distance to the typhoon center (km), y-axis represent the tangential wind speed (ms^{-1}).

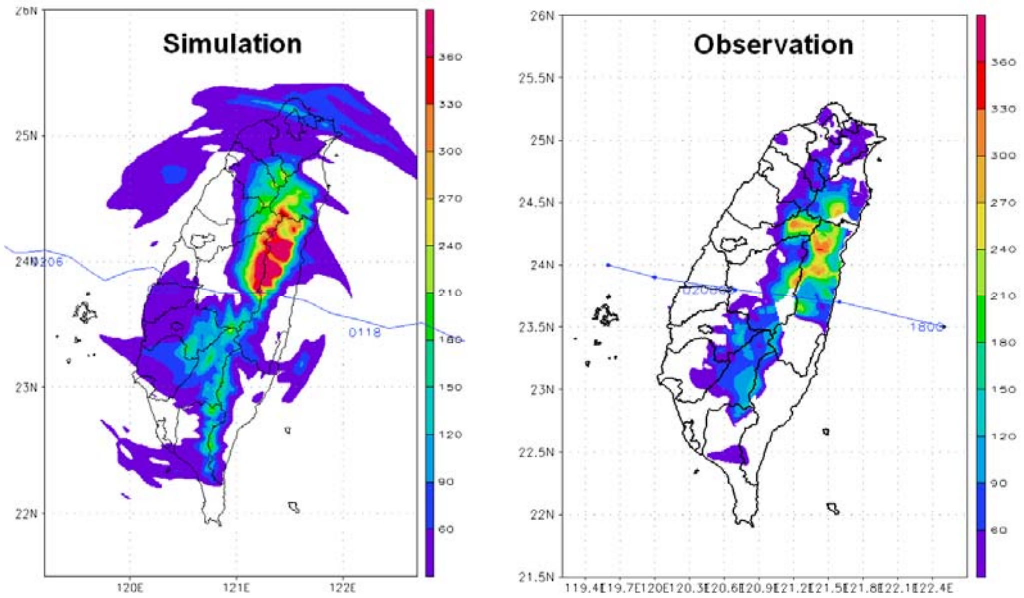

Fig. 9 Comparison of the observed accumulate rainfall during landfall period to the model simulated accumulate rainfall. Typhoon track shows in blue line.

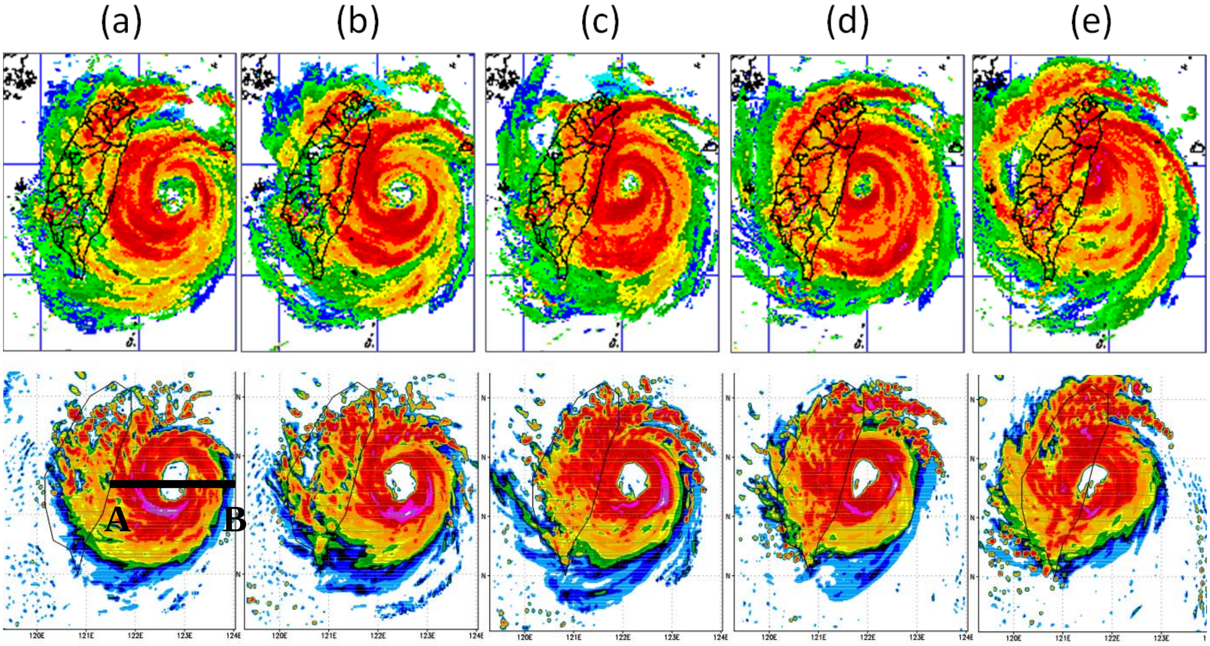

Fig. 10 Comparison of radar reflectivity (dBZ). Upper column: CWB radar composite, lower column: simulation results. (a) 4 hours before landfall, (b) 3 hours before landfall, (c) 2 hours before landfall, (d) 1 hour before landfall, (e) landfall.

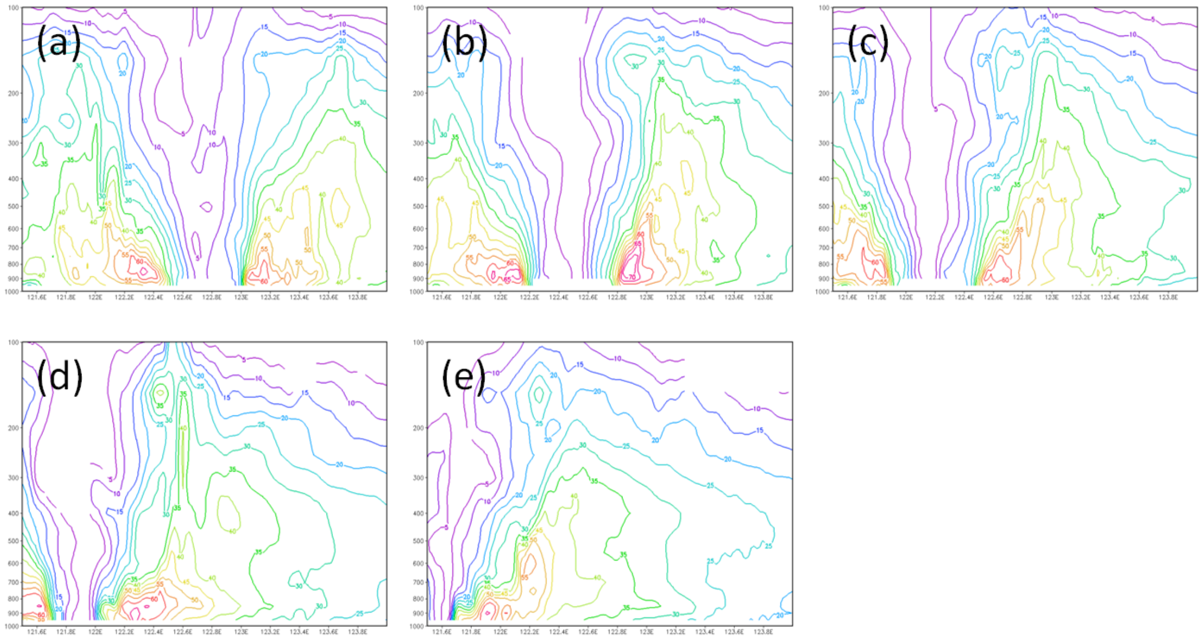

Fig. 11 Vertical cross sections of tangential winds (contour interval of 5 ms^{-1}) along line AB showed in Fig.10. (a) 4 hours before landfall, (b) 3 hours before landfall, (c) 2 hours before landfall, (d) 1 hour before landfall, (e) landfall..